



ASME Accepted Manuscript Repository

Institutional Repository Cover Sheet

André

Quintã

ASME Paper Title: Virtual test bench for the design of control strategies for water heaters

Authors: André F. Quintã; Jonathan D. Oliveira; Jorge A. F. Ferreira; Vítor A. F. Costa; N. Martins

ASME Journal Title: Journal of Thermal Science and Engineering Applications

Volume/Issue 14(5)

Date of Publication (VOR* Online) 15 Feb 2021

ASME Digital Collection URL: <https://asmedigitalcollection.asme.org/thermalscienceapplication/article-abstract/14/5/051004/1115177/Virtual-Test-Bench-for-the-Design-of-Control>

DOI: [10.1115/1.4051932](https://doi.org/10.1115/1.4051932)

*VOR (version of record)

Virtual test bench for the design of control strategies for water heaters

André F. Quintã¹

Department of Mechanical Engineering, University of Aveiro
TEMA – Centre for Mechanical Technology and Automation
Campus Universitário de Santiago, 3810-193 Aveiro, Portugal
e-mail: aquinta@ua.pt

Jonathan D. Oliveira

Department of Mechanical Engineering, University of Aveiro
Campus Universitário de Santiago, 3810-193 Aveiro, Portugal
e-mail: jonathanoliveira@ua.pt

Jorge A. F. Ferreira

Department of Mechanical Engineering, University of Aveiro
TEMA – Centre for Mechanical Technology and Automation
Campus Universitário de Santiago, 3810-193 Aveiro, Portugal
e-mail: jaff@ua.pt

Vítor A. F. Costa

Department of Mechanical Engineering, University of Aveiro
TEMA – Centre for Mechanical Technology and Automation
Campus Universitário de Santiago, 3810-193 Aveiro, Portugal
e-mail: v.costa@ua.pt

N. Martins

Department of Mechanical Engineering, University of Aveiro
TEMA – Centre for Mechanical Technology and Automation
Campus Universitário de Santiago, 3810-193 Aveiro, Portugal
e-mail: nmartins@ua.pt

ABSTRACT

An innovative methodology and a virtual test bench are proposed to support the design of water heaters' control strategies. This platform allows to speed up the development and evaluation of control systems

¹ Corresponding author.

38 *even before the existence of prototypes or real test environments. By simulating the environmental*
39 *conditions and the state of the different device components, it will be possible to detect and correct*
40 *possible initial errors in the control system design which can be time consuming and costly due to*
41 *subsequent modifications to the system or equipment components.*
42 *The architecture of the proposed system establishes four operating modes, open loop data acquisition,*
43 *real time simulation, hardware-in-the-loop simulation, and test of the complete real system, the*
44 *incorporation of these functionalities in the same platform is not reported in the literature for domestic*
45 *water heaters. The virtual test bench was designed to accommodate different water heaters including, but*
46 *not limited to, gas, electric and heat pumps, for instantaneous hot water production or including hot water*
47 *storage. The prototype of the virtual test bench is described emphasizing the hardware-in-the-loop*
48 *methodologies and embedded control. The particular case study of a tankless gas water heater is*
49 *presented implementing the different operation modes in the virtual test bench. The water heater models,*
50 *control strategies, simulation and experimental data are presented and discussed.*

51

52 *Keywords: virtual test bench, water heaters, hardware-in-the-loop simulation, embedded control, tankless*
53 *gas water heater*

54

55 **1 INTRODUCTION**

56

57 There is a growing awareness and concern with the scarceness of natural
58 resources, associated with the noticeable energy consumption increases and associated
59 harmful emissions, causing adverse effects to the environment and society. Water
60 heating represents significant part of the total buildings energy consumption, domestic
61 hot water production accounting for approximately 18% of total energy consumption in
62 the residential sector in the USA [1] and 14.5% in the EU [2]. Regulations set increasingly
63 exigent requirements on energy efficiency, nitrogen oxide emission levels, volume for

64 water heaters storage, and heat losses from hot water storage tanks, [3], bringing new
65 challenges to the manufactures.

66 The purpose of this work is to develop tools and methodologies to support the
67 implementation and evaluation of advanced control strategies for water heaters with
68 improved comfort, by reducing temperature undershoots and overshoots, in addition to
69 higher sustainability and lower environmental impact, by energy and water
70 consumption and gaseous emissions reductions.

71 Control strategies of water heaters have become increasingly complex, namely
72 with combined feedforward feedback [4,5], artificial neural networks [6,7], adaptive
73 [8,9] and predictive control [10–12], as well as the increased number of sensors and
74 actuators involved. The time available for the development and testing of new control
75 strategies in the real environment has diminished, demanding shortening of the
76 development, implementation, and test phases [13,14]. Moreover, it is necessary to
77 detect and correct possible errors in the design of the control system as earlier as
78 possible, as they become more time consuming and costly as they are only later
79 detected and corrected.

80 The development of new water heaters components, configurations, and control
81 strategies could be supported by simulation techniques such as hardware-in-the-loop-
82 simulation (HILS), without the need of the physical system (that sometimes is not yet
83 available). By simulating real conditions or even extreme conditions beyond the physical
84 limits of some of the elements, it is possible to evaluate the performance at reduced

85 costs and time, and additionally avoiding possible safety problems as, for example, with
86 combustion systems.

87 The first successful approaches of HILS were developed for flight simulation [15],
88 where the early objectives were to simulate the instruments in a secure and stable
89 cockpit. HILS systems are somehow embedded in the simulation loop, aiming to get
90 more accurate results. In HILS, part of the simulation loop is composed of computer
91 simulation, while the rest consists of hardware systems [16]. The hardware components
92 can include physical actuators and sensors and/or embedded controllers [17]. There is
93 an increasing interest in the application of HILS to improve the control of heating
94 systems [18], advanced servo pneumatic valves [19], steam plants [20], large energy
95 production facilities as thermal powerplants [21] or large hydro-power plants [22], and
96 even satellites [23]. In literature there are some previous works concerning the
97 development of test benches based on hardware-in-the-loop-simulation methodologies
98 for water heater systems. In [18], an implementation of a HILS test bench is presented
99 for heat pumps, considering space heating and tank based domestic hot water
100 production. A real heat pump is tested under real weather conditions, imposed by a
101 simulated building and emulation of a thermostat. A software-in-the-loop method is
102 implemented for test and optimize control strategies of a solar thermal system [24]. A
103 real controller of a solar thermal appliance is connected to a building simulation model
104 on Dymola environment. A test bed to improve controller's performance of ground-
105 source heat pumps is presented [25,26]. Within this system the simulated components
106 are the controller and build model. The hardware components consist of a brine water

107 heat pump and a test bed composed by heat sink, heat storage, and heat source
108 modules to emulate dynamics of external conditions and domestic hot water
109 consumption. In [27] an HILS emulation method is presented to evaluate the control
110 strategies of a hydronic radiant heating system. The authors replaced the model of a
111 hydronic network with real hardware, and the building physics is analyzed by a
112 simulation, to minimize the results uncertainties. A test bench has been realized to
113 create an interface between hardware heat pump and a TRNSYS build [28], offering the
114 possibility to simulate real ambient conditions for comparison of embedded devices
115 performance under reproducible laboratory conditions.

116 Methodologies based on HILS are state-of-the-art procedures for the evaluation
117 of embedded systems, aiming to shorten the time of the product development process.
118 However, similar works identified in the literature are mainly focused on heat pump
119 systems, applied for combined space heating and domestic hot water. Some of the
120 systems are based on simulated controllers other on simulated plant models, but none
121 incorporate in the same platform all the functionalities proposed in this work.

122 The manuscript is structured as follows, in section two the development of a
123 virtual test bench (VTB), as well as its modes of operation, is described. The proposed
124 VTB supports and accelerates the development of control strategies and algorithms for
125 thermal systems. In particular, the presented VTB prototype is designed to
126 accommodate different technologies for domestic hot water production, such as gas,
127 electric and solar water heaters and heat pumps, both for instantaneous water heating
128 or including a hot water storage tank. In section three, the particular case of a tankless

129 gas water heater (TGWH) is taken as an example, considering the VTB different
130 operating modes. It includes a presentation of the development and validation of the
131 water heater models; the design and implementation of control strategies; and the
132 implementation of HILS methodologies. In section four, simulated and experimental
133 data are presented and discussed. For validation of VTB concept, and evaluation of the
134 controller's performance, tests in all operating modes are analyzed and compared. The
135 conclusion is the fifth and final section.

136

137 **2 VIRTUAL TEST BENCH**

138

139 This section describes the definition of a framework and the developments for
140 the implementation of a platform to help the design of control strategies for water
141 heaters, referred to as virtual test bench. This platform enables the assessment of
142 advanced control strategies at the earlier stages recurring to real-time simulation
143 techniques, and in subsequent stages with the increasing introduction of hardware
144 components, until the test of the complete physical system.

145 The central components of the proposed VTB are dynamic models of water
146 heaters, compatible with real-time simulation. VTB users select which components are
147 to be tested from the model's simulation library, and which are real hardware. Water
148 heaters' models need to be able to reproduce both fast and slow dynamics of thermal
149 and fluidic components, bringing additional complexity to the implementation in real-
150 time and HILS scenarios. Some of the detailed and complex models need to be
151 simplified, and reduced models are derived for inclusion in the platform.

152 Hardware and software components were defined for the VTB, with a dedicated
153 real-time board, acquisition and interface software, instrumentation sensors, and
154 actuators for imposing environmental test conditions. An embedded control platform,
155 based on a microcontroller, with similar capabilities to the electronic control units (ECU)
156 used in appliances, is selected for the evaluation of control strategies with HILS
157 methodologies.

158

159 **2.1 Operating modes**

160

161 To assess the proposed concept and its features, the VTB must be tested through
162 different types of experiments and controllers. The design of a controller can start in a
163 fully simulated environment, afterwards, the controller is implemented in a hardware-
164 controlled device and finally, it is tested with the physical system's prototype.

165

166

167

Design of control processes requires substantial investments in time and
resources, which can be substantially reduced if the controllers' behavior can be
predicted and tested even before programming the microcontroller [29,30].

168

169

For accomplishing the different functionalities of the VTB, four operating modes
are defined as presented in Fig. 1:

170

171

172

173

174

175

The first operating method (open-loop data acquisition) enables the capability to
acquire and record data from the equipment, with data acquisition software and
hardware, in open-loop experiments. The equipment and the virtual model do not have
any type of controller, except the ones to ensure safety measures, ensuring that the
temperature and pressure limits are not exceeded. This operating mode is intended for
real-time data acquisition, with the main objective of enabling parameters estimation

176 and models' validation. By executing different experiments, in different scenarios, it is
177 possible to collect experimental data that allow models parameterization and
178 verification.

179 The second operating mode (real-time simulation) allows performing virtual
180 simulation in real-time, without any hardware for water heater or controller. The
181 dynamic model of the thermal system is controlled by a virtual model of the controller
182 while the simulation is executed in real-time. At an early stage of development, this
183 operating mode proves to be useful since it is possible to rapidly test the controllers and
184 tune their parameters.

185 In the third operating method (hardware-in-the-loop simulation), the VTB is
186 capable of performing HILS that can be either a real water heater appliance controlled
187 by a virtual model of the controller or a microcontroller platform with embedded code
188 controlling a virtual model of the system. As the main focus of this work is to support
189 control design, an embedded controller in a hardware platform is used, as the virtual
190 controller is preferred for the experimental validation of the water heater hardware
191 components. The VTB must comprise the hardware and software to simulate external
192 conditions perceived by the controller, by emulating electric signals of sensors and
193 actuators and interacting with a real-time simulation of the water heater. This mode
194 allows evaluating the controller in closer conditions of the ECU used in mass production
195 water heating appliances. Extreme environmental conditions, that are difficult or even
196 impossible to test in the real appliance, can be simulated and imposed on the controller
197 implemented in the hardware devices.

198 Finally, in the fourth operating mode (complete real system), it is possible to test
199 the actual controller in the complete real/physical system. This feature is beneficial at
200 the final phases of the test and optimization, with all components physically
201 implemented in hardware components. This is a common functionality of the
202 conventional test benches used in different engineering areas. In this operating mode,
203 the user may impose some of the environmental variables to implement automated and
204 repeated tests.

205

206 **2.2 Virtual test bench prototype**

207

208 A prototype of the VTB was developed, to test and validate the proposed
209 concept and its functionalities. This prototype was designed to accommodate different
210 domestic hot water technologies, such as gas, electric and solar water heaters, and heat
211 pumps, both for instantaneous hot water production or including a hot water storage
212 tank.

213 Besides the water heating appliance, several types of equipment were used to
214 measure and control the system's parameters. Table 1 presents the main equipment
215 used in the VTB prototype. This includes sensors for water and gas flow rates, probes for
216 multi-point water and environment temperature measurement, water pressure sensors,
217 and actuators that allow different hot water consumption regimes to be imposed in an
218 automated and replicable way.

219 Regarding the dynamic models and their parametrization, these will be quite
220 different due to the complexity and specificity of each system. The software selected for

221 modelling and simulation is based on the MATLAB/Simulink platforms and toolboxes
222 from MathWorks.

223 For the implementation of real-time simulation and HILS, a commercial digital
224 signal processing (DSP) controller board DS1104 from dSPACE was chosen. This
225 controller board supports MathWorks Simulink Coder, so the Simulink models can be
226 easily compiled to C code and optimized for real-time execution on the board. The
227 dSPACE Real-Time interface connects the Matlab, Simulink, and C code generator
228 Simulink Coder with dSPACE real-time system to form an integrated ready-to-use
229 development environment for real-time applications. The dSPACE ControlDesk software
230 is used as an interface with real-time simulation on the DS1104 board, allowing data
231 acquisition, graphic visualization and interaction with model parameters.

232 For the real discrete controller, implemented in a hardware platform, an Arduino
233 Mega is used as a low-cost controller board, to implement the functionalities of a
234 commercial ECU unit. At present time, the Arduino microcontroller is a popular low-cost
235 and highly portable solution for many engineering problems and research, so it becomes
236 a valuable resource for hardware-in-the-loop applications [31].

237 The equipment listed in Table 1 were assembled in a structure with the
238 appropriate attachments to support different water heaters. The water connections,
239 with respective instrumentation, assure the adequate supply line and allow the
240 definition of the hot water demand. The necessary electrical connections were
241 implemented for appliances power supply, instrumentation and emulation of sensors
242 signals on HILS mode. For safety reasons, when performing tests with gas water heaters

243 a carbon monoxide detector was used to prevent carbon monoxide poisoning. Fig. 2
244 presents the CAD model of the VTB, and a photo of the VTB prototype and Fig. 3
245 presents the details of the water pipe connections and some of the used sensors.

246

247 **3 CASE STUDY**

248

249 A case study was conducted for the VTB assessment. The residential and
250 commercial instantaneous gas water heater Bosch TGWH Junkers Hydro 4600 F WTD10-
251 4 KME 23 JU was selected. This non-condensation model has 22 kW thermal power, 86%
252 thermal efficiency, 8 L/min maximum water flow rate, a forced-air ventilation system,
253 and a temperature feed-forward control strategy implemented in an ECU.

254

255 **3.1 Modelling**

256

257 The central elements of the proposed VTB are mathematical models compatible
258 with real-time simulation, that describe the thermal, fluidic, and mechanical dynamics of
259 the water heater appliances.

260 The TGWH system is modeled as a lumped model in which each component is
261 implemented as a lumped element. This modelling strategy is widely used in thermal
262 systems, for example in [32,33]. Bond graphs is other popular methodology for
263 modelling thermal systems as a modular collection of reusable sub-models [34,35].
264 Bond graphs were invented by Paynte [36] and become popular with Karnoop [37].

265 Previous work [38], based on a different TGWH, was used for the development
266 and parameterization of this appliance model. In the present work, the model has been
267 simplified, with special emphasis on the energy balance equation of the control volume

268 that is the heat cell. The heat cell involves the gas burner and the heat transfer to the
 269 water in the heat exchanger. In the previous work, the heat cell also includes a second
 270 heat exchanger for condensation of the steam in the flue gases. The water and the
 271 metal (copper alloy) were assumed to be at the same temperature T , and their densities
 272 ρ are kept constant. The TGWH model is a semi-empirical nonlinear model, the energy
 273 balance equation is expressed as:

$$\frac{dT}{dt} = \frac{1}{m_w c_w + m_m c_m} (\dot{Q} + \dot{m} c_w (T_{in} - T)) \quad (1)$$

274 Indices w and m are used for water and metal respectively, and symbols m and c
 275 for mass and specific heat, respectively. The heating power (\dot{Q}) is prescribed through the
 276 flow of air+gas mixture, controlled by an electrically actuated gas valve and atmospheric
 277 or fan-forced air inlet, considering a heating efficiency η .

278 The fluidic component is described by the continuity equation in the form of Eq.
 279 (2), where P is the water pressure, β is the bulk modulus, V is the volume of the control
 280 volume and \dot{q} is the volumetric water flow rate.

$$\frac{dP}{dt} = \frac{\beta}{V} (\dot{q}_{in} - \dot{q}_{out}) \quad (2)$$

281 The Reynolds number Re is used to determine the water flow regime. The
 282 pressure drop was estimated by using the orifice equation with turbulent flow in inlet of
 283 each component. For turbulent flow, the water volumetric flow rate through an orifice is
 284 expressed by Eq. (3), where A_0 is the orifice area and C_d the discharge coefficient.

$$\dot{q} = \text{sign}(\Delta P) C_d A_0 \sqrt{\frac{2}{\rho} \Delta P} \quad (3)$$

285 The heat cell involves processes of greater complexity associated with
 286 combustion. As a semi-empirical model has been adopted, it requires parameterization
 287 using experimental results to reasonably reproduce the static and dynamic relationships
 288 between the water flow rate, the thermal power delivered to the heating cell, and the
 289 temperature of the water at the exit of the heat cell.

290 The time delay (Δt) of changes in the outlet water temperature due to the water
 291 flow is determined by the average water velocity; regarding the definition of the water
 292 mass flow rate \dot{m} , for a circular cross section pipe of radius R_i and length L it is defined
 293 as:

$$\Delta t = \frac{L \rho \pi R_i^2}{\dot{m}} \quad (4)$$

294 This time delay depends on the water flow rate. When the system is subjected to
 295 fast changes or disturbances on the water flow rate the delays vary accordingly, causing
 296 additional difficulties on the temperature controller.

297 To maintain the model's complexity within the limits required for its
 298 implementation in real-time control methodologies, these processes were empirically
 299 modelled and parameterized using laboratory experimental data. A time delay for the
 300 thermal power delivery ($t_{p\text{delay}}$) and water temperature increments at the heat cell inlet
 301 (ΔT_{in}) and outlet (ΔT_{out}) were also considered.

302 Fig. 4 presents the MATLAB/Simulink implementation of the semi-empirical
 303 model for the heat cell.

304 The model of a two-way proportional flow control valve was used to implement
 305 different water flow rates patterns, simulating changes in the hot water user demand.

306 The orifice area of the valve is determined by the spool position x and the radius R of
 307 the circular cross-section water inlet, by means of common trigonometric functions Fig.

308 5.

$$A = R^2 \cos^{-1} \left(\frac{R-x}{R} \right) - (R-x) \sqrt{2Rx - x^2} \quad (5)$$

309 The fluidic component of the model is defined by the mass conservation
 310 equation in the form of Eq. (2) for the control volume of a valve with one inlet and one
 311 outlet. Heat losses from the valve to the environment are neglected due to its small
 312 surface area. The model for the two-way proportional valve was implemented in
 313 MATLAB in a similar way as for the heat cell model.

314 The complete TGWH model was achieved by connecting the heat cell and valve
 315 Simulink blocks, as well as the controller block, which is illustrated in Fig. 6 The
 316 connections between the components of the model link their temperatures, pressures,
 317 and flow rates. The temperature and pressure values are transported from the
 318 upstream heat cell block to the downstream valve block. The outlet flow rate for the
 319 heat cell is calculated in the valve block, as a function of the spool position, and is
 320 transported to the heat cell block through an input. The controller model defines the

321 thermal power to apply, based on the temperature setpoint defined by the user, and on
322 the water inlet and outlet temperatures and flow rate.

323

324 **3.2 Control strategy**

325

326 There is a great potential to improve water heaters efficiencies and user comfort
327 by optimizing controllers' performance, and by implementing advanced control
328 strategies [39]. Combined feedforward with feedback control can significantly improve
329 the heating systems' performance over classic feedback PID control, whenever there is a
330 major disturbance that can be assessed before it impacts the process. Combined
331 feedforward feedback techniques are typically used by TGWH manufactures, and so it
332 was selected as the controller strategy for validation of the VTB prototype.

333 The TGWH appliance implements thermostatic discrete control and safety
334 functions, embedded in an ECU, based on the temperature setpoint defined by the user,
335 feedback by water temperature sensors placed at the inlet and outlet pipes, and
336 influencing the combustion air+gas mixture by actuating the electrically actuated gas
337 valve and air fan.

338 A model was developed for implementing the combined feedforward feedback
339 thermal power control as schematically represented in Fig. 7.

340 The feedforward component is based on the heat exchanger energy balance
341 equation, to calculate the predicted power required to heat water from the inlet
342 temperature up to the required setpoint temperature in steady-state conditions, for the
343 measured water flow rate, that is:

$$\dot{Q}_{FF} = \dot{m}_{in} c_w (T_{set} - T_{in}) \quad (6)$$

344 For the PID component, the feedback power is calculated based on the
345 measured heat cell outlet water temperature. The PID parameters are empirically
346 adjusted and not fully optimized.

347

348 **3.3 Model parametrization**

349

350 To enable the full use of the VTB, the water heater model must be
351 parameterized and validated with experimental data. Since several of the model's
352 parameters are unknown, the initial approach was to use the parameters from another
353 TGWH appliance [38] to parameterize the new model. A Bosch Greentherm T9800 SE
354 199 water heater, with thermal power of 58.3 kW and thermal efficiency of 99%, was
355 used for that purpose. This appliance has gas modulation, water flow regulation valves
356 (with a water bypass circuit), condensation heat exchanger, burner power segmentation
357 and forced air ventilation. This information and the provided data are summarized in
358 Table 2, which shows the parameters used in the initial simulations. It should be noted
359 that the model used in this case study has a smaller thermal capacity than the one used
360 as a reference for initial parametrization, and it is thus expected that the calibrated
361 model performs with slower dynamics.

362 Several parameters of the TGWH heat cell model were unidentified, namely the
363 mass of water (m_w) and metal (m_m) for the heat exchanger and the length (L) of the
364 internal pipes. Experimental tests were performed in the VTB to identify the unknown
365 parameters. Based on the energy balance equation, in the form of Eq. (1), and focusing

366 on the constant terms, for simplification these parameters were considered together as
367 one single undetermined term C_1 .

$$C_1 = m_w c_w + m_m c_m \quad (7)$$

368 In addition to the unknown dimensional parameters, there are parameters from
369 the empirical model component, namely the time delay for the thermal power delivery
370 (t_{Pdelay}) and water temperature increments at the heat cell inlet (ΔT_{in}) and outlet (ΔT_{out}),
371 which are assumed to be equal.

372 For collecting experimental data in open-loop tests, the thermostatic closed-loop
373 controller was disabled, and constant thermal power was forced by parameterization of
374 the ECU microcontroller. Only routines for limits monitorization remained active for
375 safety reasons.

376 Two types of tests were conducted. Steady-state regime tests were performed
377 for a combination of different constant values of thermal power and hot water flow
378 rate. Transient regime tests were made including fast changes on the water flow rate
379 under constant thermal power.

380 A multi-objective optimization method was implemented for the parameters'
381 estimation, based on the MATLAB *fminsearch* function. The cost function is based on
382 the root mean square error of a vector of experimental and simulated values that are
383 calculated in each iteration for new parameters estimations. A Simulink model of the
384 nonlinear TGWH model was used for obtaining the simulation values.

$$J = \sqrt{\frac{1}{n} \sum_{i=1}^n (Tsim_i - Texp_i)^2} \quad (8)$$

385 Using the optimization method, with experimental and simulated values, it was
386 possible to estimate the parameters of the semi-empirical heat cell model that are
387 presented in Table 3.

388 As the water heater used in this work is a non-condensing appliance, the
389 temperature increments were found negligible and removed from the model. However,
390 as the appliance used to obtain the initial parameters has a condensation heat
391 exchanger, the temperature increments revealed to be relevant and cannot be ignored.

392

393 **3.4 Hardware-in-the-loop simulation**

394

395 The previously described calibrated TGWH model was implemented in Simulink
396 and compiled for real-time simulation in the dSPACE DS1104 board. For performing
397 closed-loop simulation in real-time, the combined feedforward feedback control
398 strategy was also implemented in Simulink and connected to the TGWH model blocks.
399 For the implementation of HILS methodologies, a low-cost Arduino based platform was
400 used for the application of the embedded controller. The Arduino MEGA was selected to
401 replace, in a more realistic way, the microcontroller used in the ECU of commercial
402 TGWH appliances. The ECU implemented in the TGWH used in this work is based on a
403 Renesas 16-bit microcontroller, with approximately 250 ms program cycle time, which

404 implies a significant time delay in the controller reaction. The hardware and software
405 implemented for the HILS framework are schematically presented in Fig. 8.

406 The integration of the water heater model (implemented in the dSPACE board)
407 with the embedded controller (implemented in the Arduino board) was achieved with
408 analogue voltage electric signals. The dSPACE DS1104 controller board is built with the
409 embedded 64-bit MPC8240 processor, a sampling frequency of 1 kHz was used for real
410 time simulations. This board has eight analogue inputs, four with 12 bits and four with
411 16 bits, with ± 10 V single-ended range and eight 16 bits voltage analogic outputs, also
412 with ± 10 V. For the Arduino, the analogue inputs are in the 0 to 5V range, so not the full
413 range of the dSPACE signals is used, but as the Arduino ADC resolution is only 10-bit, this
414 is not a problem. The Arduino PWM outputs are converted to analogue voltages by
415 using discrete RC low pass filters.

416 The values for the inlet and outlet water temperatures and water flow rate are
417 sent from the virtual model, as dSPACE output signals, connected to the Arduino inputs.
418 The output of the controller is the thermal power to apply to the system, defined as
419 Arduino output connected to the dSPACE input. The calibration of the electric signals
420 was performed in steady-state for the minimum and maximum input and output values,
421 for compensating RC voltage drop and acquisition errors. The diagnostic of the Arduino
422 program was implemented with serial communication to the PC.

423 The action control signal is determined in the Arduino embedded program, by
424 implementing the combined feedforward feedback control strategy. First, water
425 temperature and flow rate values are read from the analogue inputs and converted to

426 an appropriate scale. Second, mathematical expressions are applied to determine the
427 theoretical and effective thermal power including saturation functions. Third, the
428 thermal power error is determined as the difference between theoretical and effective
429 thermal powers, this error is the PID controller input. The fourth step consists of
430 calculating the PID terms, which are summed and saturation is implemented. Finally, the
431 PID term is added to the result obtained from the theoretical thermal power, saturated,
432 and converted to the scale of the output signal.

433

434 **4 RESULTS AND DISCUSSION**

435

436 Following the defined methodology, tests were carried out in the VTB four

437 modes of operation to evaluate its capabilities for the TGWH case study. The

438 experimental and simulated results are presented and discussed in this section.

439

440 **4.1 Data acquisition and model parameterization**

441

442 As previously referred, experimental tests were conducted in an open-loop, both

443 in steady and in unsteady regimes, to collect data for the parameterization of the heat

444 cell model. A multi-objective optimization routine was used to obtain the calibrated

445 model. For model validation purposes, a separate set of laboratory tests was performed,

446 to gather experimental data, different from the data used for parameterization

447 purposes. To evaluate the model's performance, several simulations were performed

448 under different scenarios, and the predicted values compared with the measured data.

449 Steady-state experiments were performed with constant inputs for the inlet

450 temperature, water flow rate and thermal power, and after stabilization, the average

451 outlet water temperature was recorded. For a scenario of constant minimum thermal
452 power, without extinguishing the burner, experimental and simulated steady-state
453 outlet water temperatures were recorded for different values of constant water flow
454 rate (Fig. 9). The experimental and simulated results are in very good agreement, with
455 just a small discrepancy for the smaller flow rates.

456 Fig. 10, presents the comparison between experimental and simulated results
457 for open-loop tests in a scenario of constant water flow rate, and a sequence of fast
458 changes in the applied thermal power (32%, 50% and 100%). The simulation results are
459 in very good agreement, even if overlapping the experimental results in most cases. In
460 what concerns the steady-state values, they are essentially coincident, even if small
461 differences are observed during the transient segments.

462 The calibrated TGWH model was considered reliable for this work, as the
463 observed differences between simulated and experimental results fall between
464 acceptable limits. A script was used to obtain the steady-state simulated values, for the
465 full range of water flow rate and thermal powers. Fig. 11 presents the simulated outlet
466 water temperature for the combination of inputs. The observable upper plane on the
467 left of Fig. 11 is due to a temperature saturation in the model, with values higher than
468 the safety appliance limits.

469

470 **4.2 Real-time simulation**

471

472 After the calibration and validation of the TGWH model is possible to go some
473 steps forward and perform close loop tests with thermostatic control. In this VTB

474 operating mode, it is possible to perform tuning tasks and evaluation of controller
475 performance by executing the real-time simulation.

476 One of the disadvantages of instantaneous water heaters is the difficulty to
477 maintain a constant hot water temperature as sudden changes occur in the hot water
478 demand. One way to assess the controller's performance is to measure water
479 temperature overshoots and undershoots when the hot water flow rate suddenly
480 changes.

481 Fig. 12 presents the simulation results for a sequence of fast changes in the hot
482 water flow rate demand. Even though the controller can respond and return to the
483 setpoint temperature after the disturbance, some significant overshoots and
484 undershoots are still noticed, which is a handicap for the user comfort.

485

486 **4.3 HILS with microcontroller**

487

488 After tuning the controller parameters, it is possible to implement and assess
489 the control strategy in an embedded controller, in a closer way as implemented in the
490 real ECU microcontroller.

491 In Fig. 13 is possible to observe the controller performance in the embedded
492 controller, with HILS, versus the real-time simulation, for fast changes on the hot water
493 demand. Both temperature and thermal power are almost perfectly overlapping. A
494 slight discrepancy in the outlet temperature is observed after the 500 s time mark and
495 an almost imperceptible oscillation due to the noise in the acquisition process.

496

4.4 Tests with the complete system

497

498

499

500

501

502

503

504

505

506

After validation of the controller in an embedded environment it is possible to advance to the last VTB operating mode, which corresponds to conduct tests with the complete system. The control strategy and tuning parameters can be integrated into the source code of the appliance ECU. This task needs to be performed and validated by the manufacturer for safety reasons, and to assure that the appliance fully complies with the required standards. For the fourth operating mode of the VTB, tests were performed with the complete real system, without any simulated component, yet without the updated ECU code.

507

508

509

510

511

512

513

514

515

516

517

518

519

Fig. 14, presents the experimental results for a test of the TGWH a in close loop under a very demanding sequence of fast changes in the hot water flow rate. For smaller water flow changes the observed temperature overshoots and undershoots are acceptable. However, when submitted to a more demanding situation, after the 530 s time mark, the controller is not able of providing suitable temperatures for the user's comfort and becomes unstable after 600 s. The high-water temperatures of 55 °C for a setpoint of 40°C are not acceptable and can even become a safety issue. This is due to the relatively slow dynamics of the heat exchanger, and to the system varying time delays, causing temperature changes on the outlet hot water that depend heavily on the hot water flow rate and on the length of the pipes where it is flowing. The registered data confirm that more research is needed to develop and validate advanced control strategies and support tools, as the proposed VTB, for improved control design and validation.

520

521 **5 CONCLUSIONS**

522

523

524

525

526

527

528

529

530

531

532

533

534

535

536

537

538

539

540

541

542

543

The methodology and the virtual test bench presented in this work are important achievements enabling faster development of control strategies for water heaters. To the best of the authors' knowledge, there are no successful implementations of test benches with similar methodology and capabilities for this field in the literature.

A prototype of the VTB was developed and validated, through experimental and simulated tests in four operating modes, using a TGWH as a case study. By applying HILS methodologies, the performance of a combined feedforward feedback control strategy was evaluated in an embedded controller, using both simulation and the real water heater appliance.

Laboratory tests revealed some limitations of the present controller, reinforcing the importance of developing improved controllers. Accurate testing and validation of complex controllers are increasingly important for water heaters manufacturers. The presented concept supported the development and evaluation of new (predictive and adaptive) advanced control strategies for domestic hot water appliances under the scope of the Smart Green Homes project. This platform will be a major factor to shorten the development cycle and allow the development of increased performance controllers.

The proposed VTB also presents a great potential for use in the academic environment, namely in the fields of modelling, simulation and controllers design for thermal systems, as well as in the experimental application of HILS concepts.

544

545 **FUNDING**

546

547

548

549

550

551

552

553

554

555

556

557

The present study was developed under the scope of the Smart Green Homes Project [POCI-01-0247 FEDER-007678], a co-promotion between Bosch Termotecnologia S.A. and the University of Aveiro. It is financed by Portugal 2020, under the Competitiveness and Internationalization Operational Program, and by the European Regional Development Fund. André Quintã acknowledges the financial support from the Foundation for Science and Technology (FCT) (SFRH/BD/145713/2019). Thanks are also due to the support by the projects UIDB/00481/2020 and UIDP/00481/2020 - FCT - Fundação para a Ciência e a Tecnologia; and CENTRO-01-0145-FEDER-022083 - Centro Portugal Regional Operational Programme (Centro2020), under the PORTUGAL 2020 Partnership Agreement, through the European Regional Development Fund.

558 **NOMENCLATURE**
559

A	area
c_p	specific heat
C_1	auxiliar constant for calculation
C_d	discharge coefficient
L	length
m	mass
\dot{m}	mass flow rate
P	pressure
\dot{q}	volumetric flow rate
\dot{Q}	heating power
R	radius
Re	Reynolds number
t	time
T	temperature
V	volume
x	position
β	bulk modulus
ρ	density

η efficiency

560

561 **REFERENCES**

562

563 [1] Energy Information Administration, 2017, *Residential Energy Consumption Survey*
564 *(RECS) 2015 Technical Documentation Summary*.

565

566 [2] Eurostat European Commission, 2017, *Energy, Transport and Environment*
567 *Indicators*, Statistical Office of the European Union.

568

569 [3] 2013, "Commission Regulation (EU) No. 814/2013 of 2 August 2013 Implementing
570 Directive 2009/125/EC of the European Parliament and of the Council with
571 Regard to Ecodesign Requirements for Water Heaters and Hot Water Storage
572 Tanks."

573

574 [4] David Yuill, 2008, *Development of an Accurate Feed-Forward Temperature Control*
575 *Tankless Water Heater*, Pittsburgh, PA, and Morgantown, WV.

576

577 [5] Costa, V., Ferreira, J., and Guilherme, D., 2016, "Modeling and Simulation of
578 Tankless Gas Water Heaters to Reduce Temperature Overshoots and
579 Undershoots," *Proceedings of the 12th International Conference on Heat Transfer,*
580 *Fluid Mechanics and Thermodynamics (HEFAT 2016)*, HEFAT, Málaga, Spain, pp.
581 1404–1409.

582

583 [6] Laurencio-Molina, J. C., and Salazar-Garcia, C., 2018, "Design of an Artificial
584 Neural Network Controller for a Tankless Water Heater By Using a Low-Profile
585 Embedded System," *2018 IEEE International Work Conference on Bioinspired*
586 *Intelligence (IWOBI)*, IEEE, pp. 1–9.

587

588 [7] Xu, K., Qiu, X., Li, X., and Xu, Y., 2008, "A Dynamic Neuro-Fuzzy Controller for Gas-
589 Fired Water Heater," *2008 Fourth International Conference on Natural*
590 *Computation*, IEEE, pp. 240–244.

591

592 [8] Bobál, V., Kubalčík, M., Dostál, P., Novák, J., Bobal, V., Kubalčík, M., Dostál, P., and
593 Novák, J., 2014, "Adaptive Predictive Control of Laboratory Heat Exchanger,"
594 *WSEAS Trans. Syst.*, **13**(Multi-models for Complex Technological Systems), pp.
595 470–481.

596

597 [9] Haissig, C., and Woessner, M., 2000, "An Adaptive Fuzzy Algorithm for Domestic
598 Hot Water Temperature Control of a Combi-Boiler," *HVAC&R Res.*, **6**(2), pp. 117–
599 134.

600

601 [10] Henze, G., Yuill, D., and Coward, A., 2009, "Development of a Model Predictive
602 Controller for Tankless Water Heaters," *HVAC&R Res.*, **15**(1), pp. 3–23.

603

604 [11] Wanjiru, E. M., Sichilalu, S. M., and Xia, X., 2017, "Model Predictive Control of

- 605 Heat Pump Water Heater-Instantaneous Shower Powered with Integrated
606 Renewable-Grid Energy Systems,” *Appl. Energy*, **204**, pp. 1333–1346.
607
- 608 [12] Rodrigues, E. M. G., Godina, R., Pouresmaeil, E., Ferreira, J. R., and Catalão, J. P.
609 S., 2017, “Domestic Appliances Energy Optimization with Model Predictive
610 Control,” *Energy Convers. Manag.*, **142**, pp. 402–413.
611
- 612 [13] Lauss, G., Majstorovic, D., Leimgruber, F., Gagrica, O., Bründlinger, R., Morar, I.,
613 Miletic, Z., and Celanovic, N., 2017, *Development of a Controller-Hardware-in-the-
614 Loop (CHIL) Toolbox Applied for Pre-Certification Services for Grid-Connected PV
615 Inverters According to the State-of-the-Art BDEW RL Guideline and FGW TR3
616 Standard*.
617
- 618 [14] Gurov, D., Herber, P., and Schaefer, I., 2020, “Automated Verification of
619 Embedded Control Software BT - Leveraging Applications of Formal Methods,
620 Verification and Validation: Applications,” T. Margaria, and B. Steffen, eds.,
621 Springer International Publishing, Cham, pp. 235–239.
622
- 623 [15] Jeon, C., 2015, “The Virtual Flier: The Link Trainer, Flight Simulation, and Pilot
624 Identity,” *Technol. Cult.*, **56**(1), pp. 28–53.
625
- 626 [16] Xue, D., and Chen, Y., 2014, *System Simulation Techniques with MATLAB and
627 Simulink*, John Wiley & Sons, Ltd.
628
- 629 [17] Sporr, A., and Lauermann, M., 2020, “Controller-in-the-Loop - New Ways of
630 Optimizing Costs and Quality of Heat Pump Systems,” *Heat Pump. Technol. Mag.*,
631 **39**(3).
632
- 633 [18] Tejeda De La Cruz, A., Riviere, P., Marchio, D., Cauret, O., and Milu, A., 2017,
634 “Hardware in the Loop Test Bench Using Modelica: A Platform to Test and
635 Improve the Control of Heating Systems,” *Appl. Energy*, **188**, pp. 107–120.
636
- 637 [19] Pugi, L., Galardi, E., Pallini, G., Paolucci, L., and Lucchesi, N., 2016, “Design and
638 Testing of a Pulley and Cable Actuator for Large Ball Valves,” *Proc. Inst. Mech.
639 Eng. Part I J. Syst. Control Eng.*, **230**(7), pp. 622–639.
640
- 641 [20] Pugi, L., Galardi, E., Carcasci, C., Rindi, A., and Lucchesi, N., 2015, “Preliminary
642 Design and Validation of a Real Time Model for Hardware in the Loop Testing of
643 Bypass Valve Actuation System,” *Energy Convers. Manag.*, **92**, pp. 366–384.
644
- 645 [21] Iacob, M., and Andreescu, G.-D., 2011, “Real-Time Hardware-in-the-Loop Test
646 Platform for Thermal Power Plant Control Systems,” *2011 IEEE 9th International
647 Symposium on Intelligent Systems and Informatics*, IEEE, pp. 495–500.
648

- 649 [22] ZaeV, E., Tuneski, A., Babunski, D., Trajkovski, L., Nospal, A., and Rath, G., 2012,
650 "Hydro Power Plant Governor Testing Using Hardware-in-the-Loop Simulation,"
651 *Proceedings of the 2012 Mediterranean Conference on Embedded Computing*
652 *(MECO 2012)*, Bar, Montenegro, pp. 271–274.
653
- 654 [23] Rodrigues, R., Murilo, A., Lopes, R. V., and Souza, L. C. G. De, 2019, "Hardware in
655 the Loop Simulation for Model Predictive Control Applied to Satellite Attitude
656 Control," *IEEE Access*, **7**, pp. 157401–157416.
657
- 658 [24] Huber, M., Bons, C., and Müller, D., 2014, "Exergetic Evaluation of Solar
659 Controller Using Software-in-the-Loop Method," *Energy Procedia*, **48**, pp. 850–
660 857.
661
- 662 [25] El-Baz, W., Mayerhofer, L., Tzscheutschler, P., and Wagner, U., 2018, "Hardware
663 in the Loop Real-Time Simulation for Heating Systems: Model Validation and
664 Dynamics Analysis," *Energies*, **11**(11), p. 3159.
665
- 666 [26] El-Baz, W., Tzscheutschler, P., and Wagner, U., 2018, "Experimental Study and
667 Modeling of Ground-Source Heat Pumps with Combi-Storage in Buildings,"
668 *Energies*, **11**(5), p. 1174.
669
- 670 [27] Rhee, K. N., Yeo, M. S., and Kim, K. W., 2011, "Evaluation of the Control
671 Performance of Hydronic Radiant Heating Systems Based on the Emulation Using
672 Hardware-in-the-Loop Simulation," *Build. Environ.*, **46**(10), pp. 2012–2022.
673
- 674 [28] Schoberer, T., Weyr, J., Steindl, G., Görtler, G., and Stutterecker, W., 2019,
675 "Comparison of the Energy Performance of a Heat Pump under Various
676 Conditions by Using a Hardware-in-the-Loop (HIL) Test Method," *Appl. Mech.*
677 *Mater.*, **887**, pp. 622–632.
678
- 679 [29] Nguyen, V. H., Nguyen, T. L., Tran, Q. T., Besanger, Y., and Caire, R., 2020,
680 "Integration of SCADA Services and Power-Hardware-in-the-Loop Technique in
681 Cross-Infrastructure Holistic Tests of Cyber-Physical Energy Systems," *IEEE Trans.*
682 *Ind. Appl.*, **56**(6), pp. 7099–7108.
683
- 684 [30] Thornton, M., Motalleb, M., Smidt, H., Branigan, J., Siano, P., and Ghorbani, R.,
685 2018, "Internet-of-Things Hardware-in-the-Loop Simulation Architecture for
686 Providing Frequency Regulation With Demand Response," *IEEE Trans. Ind.*
687 *Informatics*, **14**(11), pp. 5020–5028.
688
- 689 [31] Tejado, I., Serrano, J., Pérez, E., Torres, D., and Vinagre, B. M., 2016, "Low-Cost
690 Hardware-in-the-Loop Testbed of a Mobile Robot to Support Learning in
691 Automatic Control and Robotics," *IFAC-PapersOnLine*, **49**(6), pp. 242–247.
692

- 693 [32] Pugi, L., Galardi, E., Carcasci, C., and Lucchesi, N., 2017, "Hardware-in-the-Loop
694 Testing of Bypass Valve Actuation System: Design and Validation of a Simplified
695 Real Time Model," *Proc. Inst. Mech. Eng. Part E J. Process Mech. Eng.*, **231**(2), pp.
696 212–235.
697
- 698 [33] Bianchi, M., Branchini, L., De Pascale, A., Melino, F., Ottaviano, S., Peretto, A., and
699 Torricelli, N., 2019, "Application and Comparison of Semi-Empirical Models for
700 Performance Prediction of a KW-Size Reciprocating Piston Expander," *Appl.*
701 *Energy*, **249**, pp. 143–156.
702
- 703 [34] D'Adamio, P., Galardi, E., Meli, E., Nocciolini, D., Pugi, L., and Rindi, A., 2017,
704 "Real-Time Modeling, Control and Optimization of Turbo-Machinery Auxiliary
705 Plants," *Proc. Inst. Mech. Eng. Part I J. Syst. Control Eng.*, **232**(3), pp. 244–257.
706
- 707 [35] Gerard, A., Tahir, A., Tankari, M., and Lefebvre, G., 2017, *Modelling Bond Graph*
708 *of a Thermal Solar Water Heater for Thermal Comfort in a Building*.
709
- 710 [36] Paynter, H. M., 1961, *Analysis and Design of Engineering Systems*, MIT press.
711
- 712 [37] Karnopp, D., Rosenberg, R., and Perelson, A. S., 1976, "System Dynamics: A
713 Unified Approach," *IEEE Trans. Syst. Man. Cybern.*, **SMC-6**(10), p. 724.
714
- 715 [38] Quintã, A. F., Ferreira, J. A. F. F., Ramos, A., Martins, N. A. D. D., and Costa, V. A. F.
716 F., 2019, "Simulation Models for Tankless Gas Water Heaters," *Appl. Therm. Eng.*,
717 **148**, pp. 944–952.
718
- 719 [39] Jin, X., Maguire, J., and Christensen, D., 2014, "Model Predictive Control of Heat
720 Pump Water Heaters for Energy Efficiency," *ACEEE Summer Study on Energy*
721 *Efficiency in Buildings*.
722
- 723 [40] Ehtiwesh, I. A. S., Quintã, A. F., and Ferreira, J. A. F., 2021, "Predictive Control
724 Strategies for Optimizing Temperature Stability in Instantaneous Hot Water
725 Systems," *Sci. Technol. Built Environ.*, **27**(5), pp. 679–690.
726

727
728

Figure Captions List

- Fig. 1 Layout of the virtual test bench for the four different operating modes
- Fig. 2 VTB CAD model and prototype's photo
- Fig. 3 Details of VTB water connections and sensors
- Fig. 4 MATLAB/Simulink model diagram for heat cell
- Fig. 5 Valve orifice area schematic
- Fig. 6 Simulink model diagram of TGWH
- Fig. 7 Schematic of the combined feedforward feedback thermal power controller [40]
- Fig. 8 Hardware and software HILS framework
- Fig. 9 Experimental and simulated results (water temperature versus flow rate) for minimum thermal power
- Fig. 10 Experimental and simulated results (water temperature) for a sequence of thermal power changes
- Fig. 11 Simulated results (water temperature, water flow rate and thermal power)
- Fig. 12 Closed-loop real-time simulation results
- Fig. 13 Embedded HILS vs real-time simulation results
- Fig. 14 TGWH controlled by the ECU implemented in the device experience

729

730 **Table Caption List**

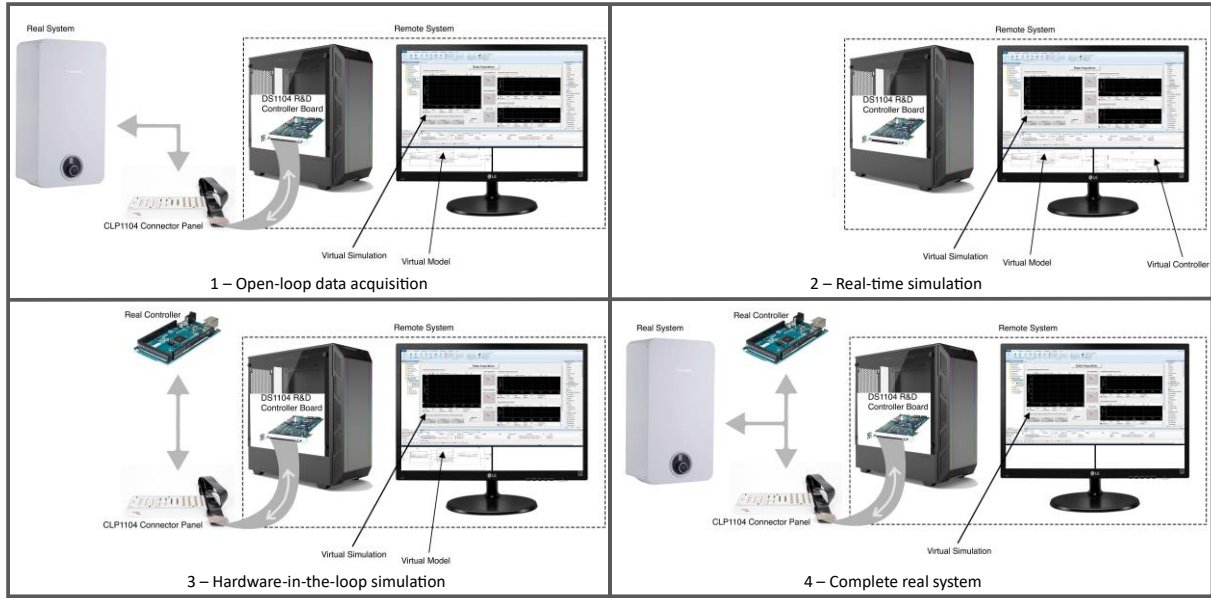
731

Table 1 Prototype instrumentation equipment

Table 2 TGWH initial parameters [38]

Table 3 TGWH model parameters

732



733

734

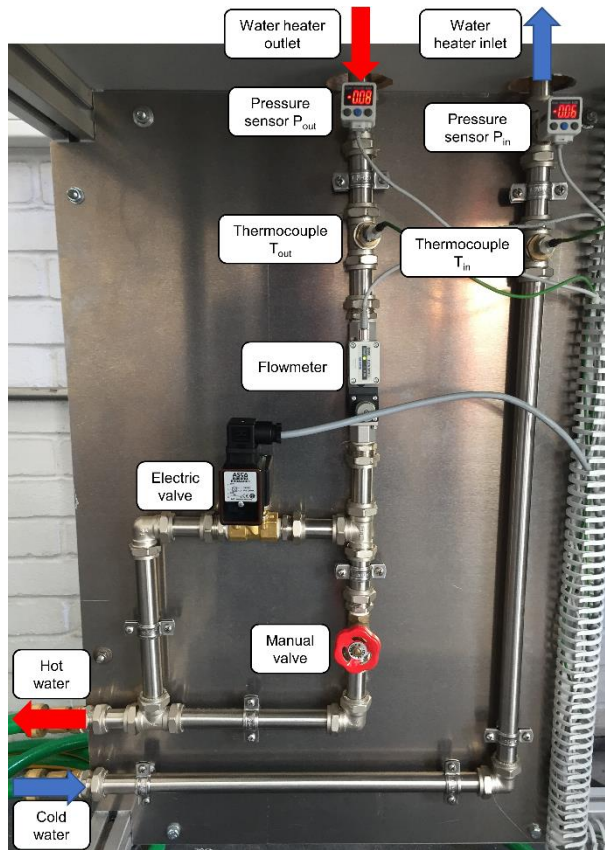
Fig. 1 Layout of the virtual test bench for the four different operating modes



735

736

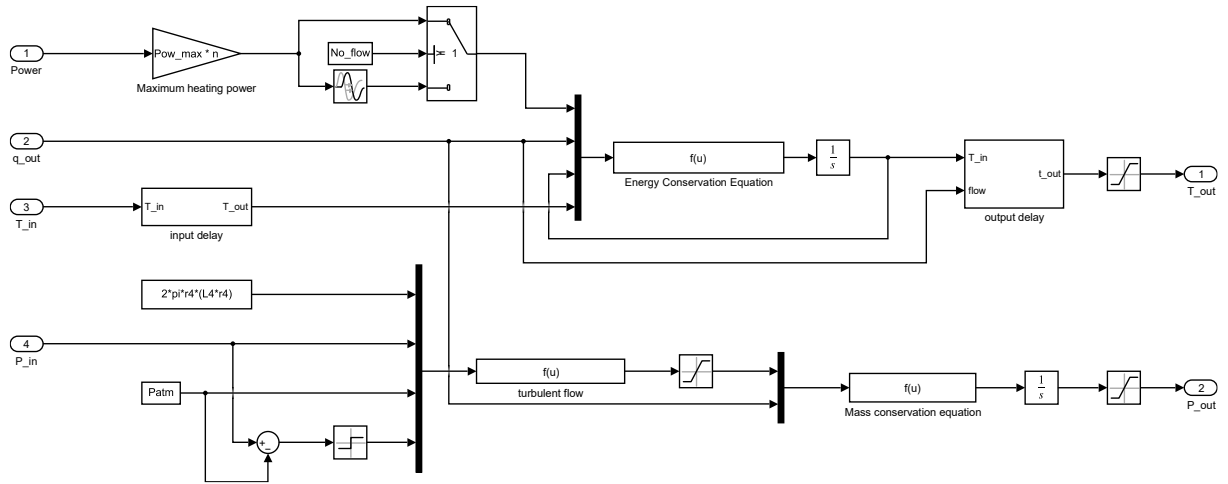
Fig. 2 VTB CAD model and prototype's photo



737

738

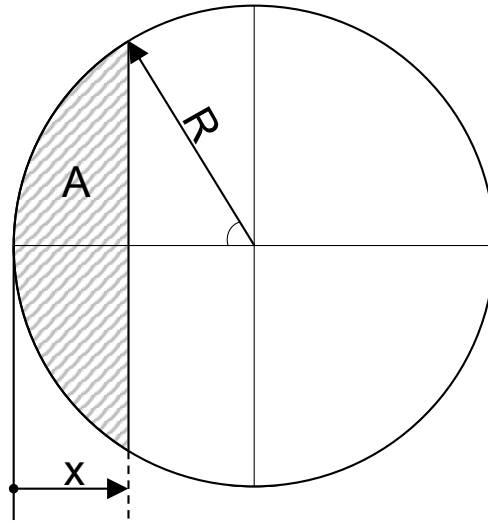
Fig. 3 Details of VTB water connections and sensors



739

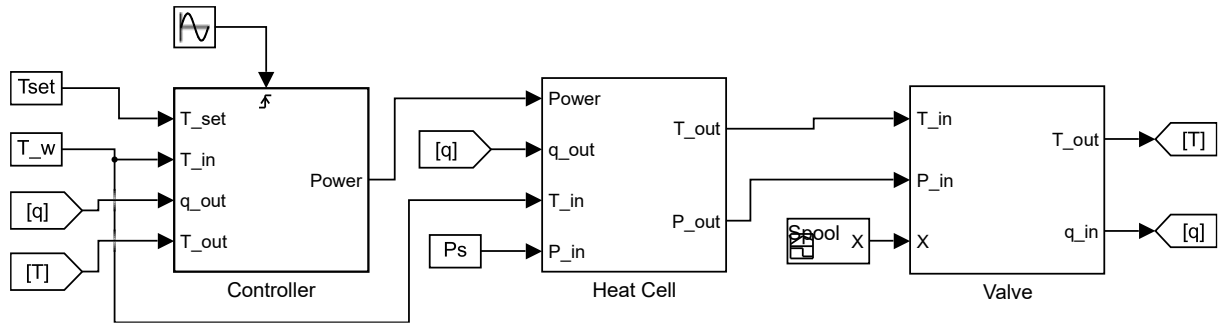
740

Fig. 4 MATLAB/Simulink model diagram for heat cell



741
742

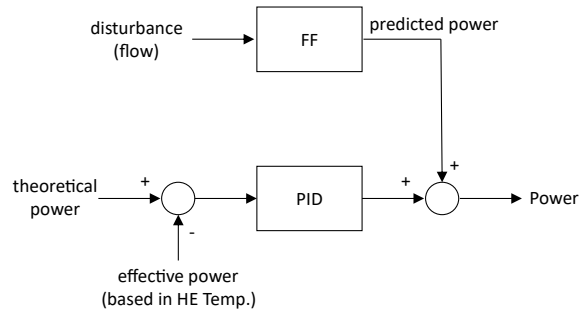
Fig. 5 Valve orifice area schematic



743

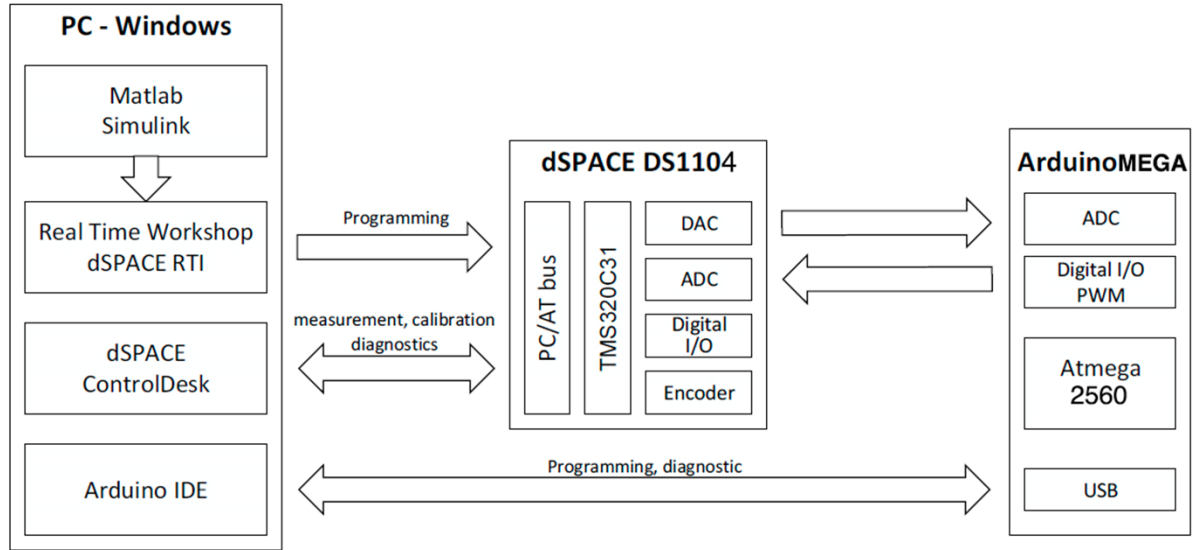
744

Fig. 6 Simulink model diagram of TGWH



745

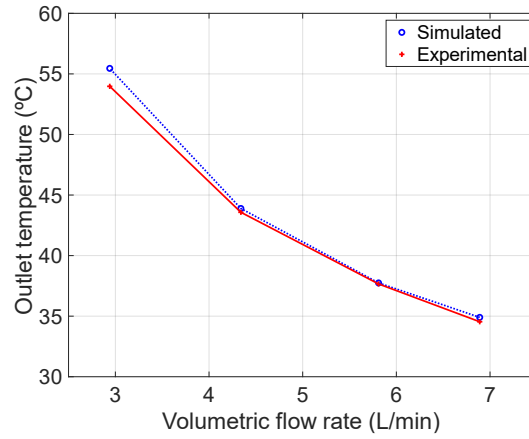
746 **Fig. 7 Schematic of the combined feedforward feedback thermal power controller [40]**



747

748

Fig. 8 Hardware and software HILS framework

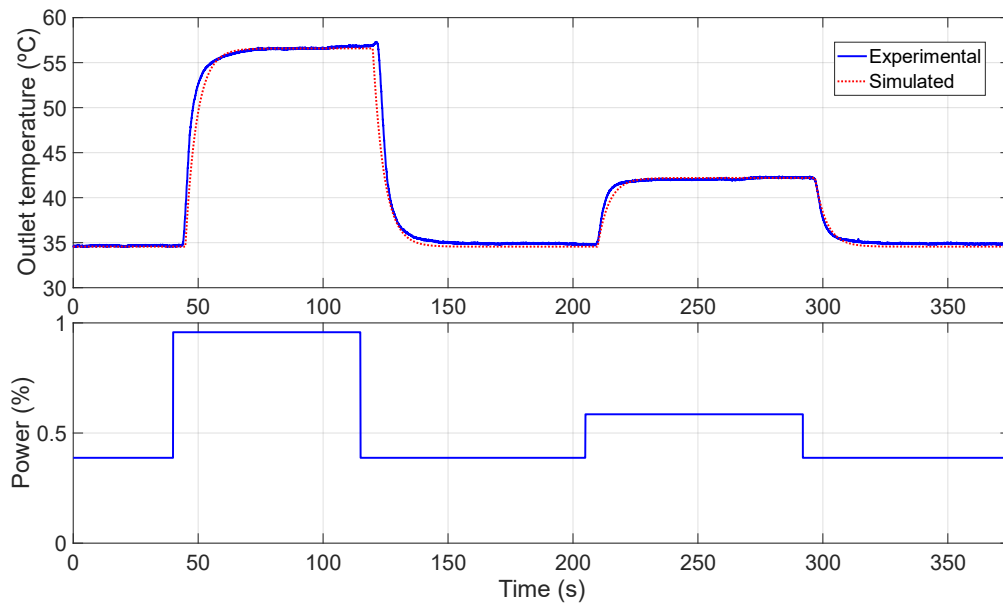


749

750

751

Fig. 9 Experimental and simulated results (water temperature versus flow rate) for minimum thermal power



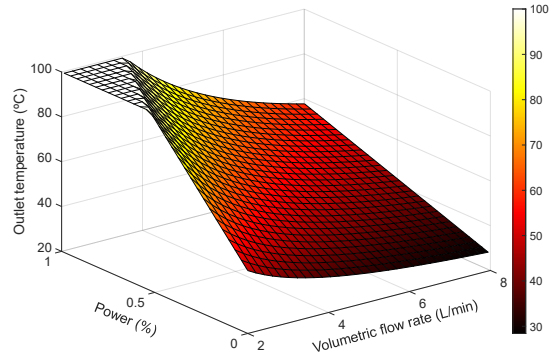
752

753

Fig. 10 Experimental and simulated results (water temperature) for a sequence of

754

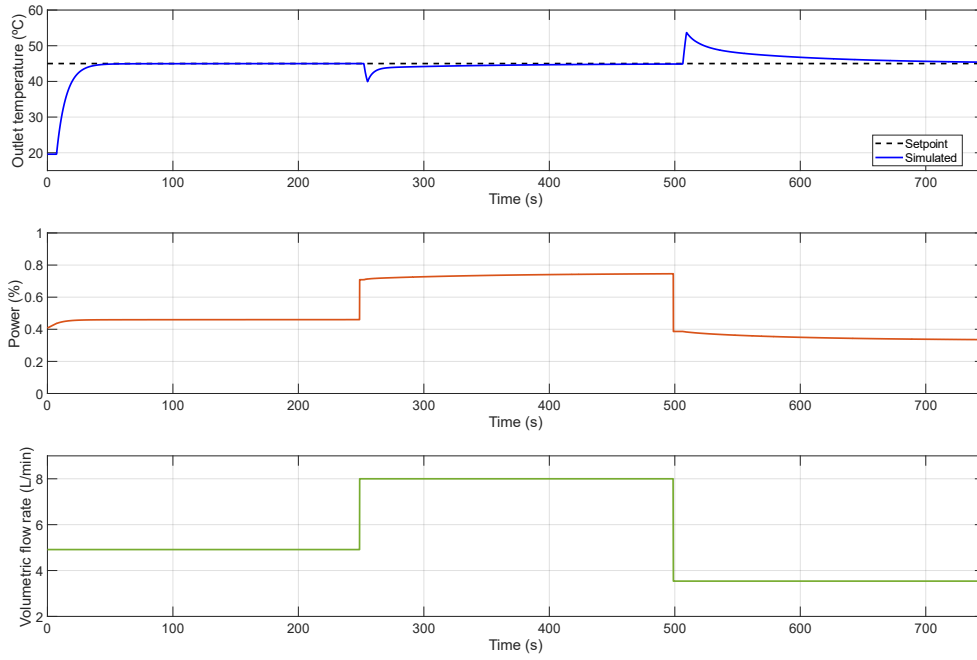
thermal power changes



755

756

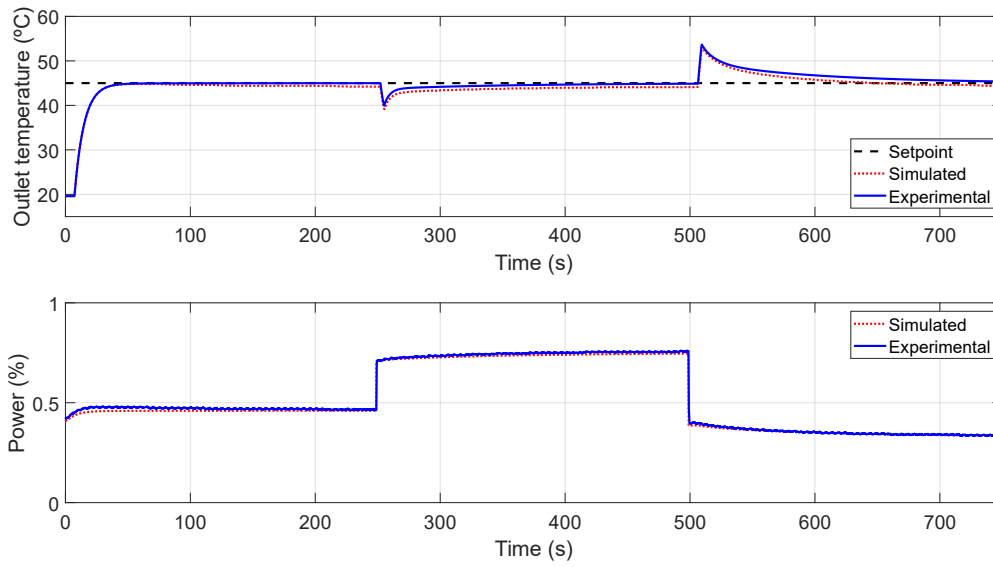
Fig. 11 Simulated results (water temperature, water flow rate and thermal power)



757

758

Fig. 12 Closed-loop real-time simulation results

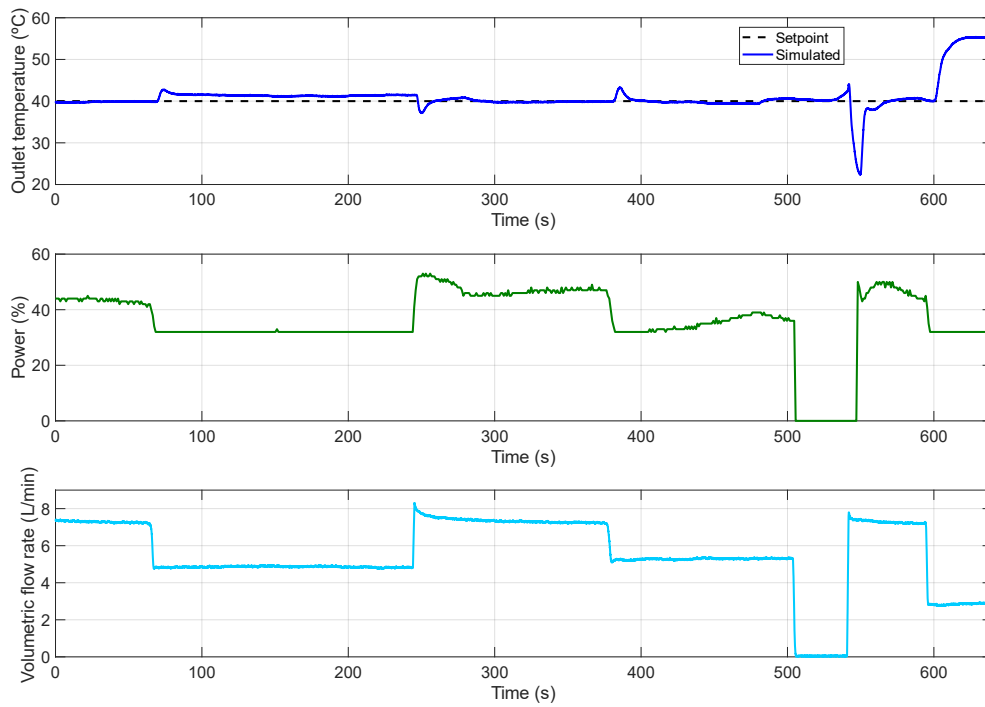


759

760

Fig. 13 Embedded HILS vs real-time simulation results

761



762

763

Fig. 14 TGWH controlled by the ECU implemented in the device experience

764

Table 1 Prototype instrumentation equipment

Quantity	Components	Manufacturer part number
1	Carbon monoxide detector	Honeywell XC100
2	K-type thermocouple, ± 2.5 °C	Tekon BT.MiK.1.2.1,5.50.PVC2,5.0
1	RTD PT100 sensor, class A, ± 0.35 °C	Tekon BR.Pt1.1C.4.3.100.MFA2.0
2	Pressure sensor, 0-10 bar, $\pm 2,5\%$	SMC ISE80-F02-T-X501
1	Water flow meter, 2 to 16 L/min, $\pm 0,5\%$	SMC PF3W740S-F06-EN-M
1	Gas mass flow meter, 0-20 L _n /min, $\pm 0,5\%$	Bronkhorst F-111AC
1	Proportional solenoid valve	ASCO SCG203B002
1	Manual flow control valve	

765

766

Table 2 TGWH initial parameters [38]

Section	Parameters	Value
Water circuit	Inlet water temperature	16 °C
	Water supply pressure	3×10^5 Pa
	Effective bulk modulus (air+water mixture)	5×10^8 Pa
Valve	Orifice radius	4×10^{-3} m
	Discharge coefficient	0.7
Heat cell	Power time delay	2.5 s
	Temperature increment at the input	1.25 °C
	Temperature increment at the output	1.25 °C
	Water mass	2 kg
	Cooper alloy mass	2 kg
	Orifice radius	8×10^{-3} m
	Water circuit length	2.2 m

767

768

Table 3 TGWH model parameters

Parameter	Value	Description
C_1	2218.1 J/°C	Auxiliar constant for calculation
ΔT_{in}	0 °C	Inlet temperature increment
ΔT_{out}	0 °C	Outlet temperature increment
t_{Pdelay}	2.9 s	Power delivery time delay
L	2.2 m	Heat exchanger pipe length

769